pretation of the permeation characteristics of the multi-component bilayer film. Discontinuous jump of P at T_c is ascribable to greater gas mobility in the liquid-crystalline phase of the hydrocarbon component, and the jump becomes larger as the hydrocarbon domain is enlarged.

Concluding Remarks

Multicomponent bilayer membranes can be immobilized in the form of PVA composite films. The DSC and XPS data indicate that the hydrocarbon and fluorocarbon bilayer components are phase-separated and that the fluorocarbon component is concentrated near the film surface. These component distributions produce favorable effects on permselectivity of O_2 gas. The selectivity (P_{O_2}/P_{N_2}) is apparently determined by the surface monolayer (or layers close to the surface) of the fluorocarbon component, and the permeability is promoted by the presence of large domains of the fluid (in the liquid-crystalline state) hydrocarbon bilayer.

(4) Kunitake, T.; Tsuge, A.; Nakashima, N. *Chem. Lett.* 1984, 1783.
(5) Kunitake, T.; Higashi, N.; Kajiyama, T. *Chem. Lett.* 1984, 717.
(6) Takahara, A.; Kajiyama, T., personal communication.
(7) Kunitake, T.; Tawaki, S.; Nakashima, N. *Bull. Chem. Soc. Jpn.* 1983, 56, 3235.
(8) Kunitake, T.; Higashi, N. *J. Am. Chem. Soc.* 1985, 107, 692.
(9) Kunitake, T.; Asakuma, S.; Higashi, N.; Nakashima, N. *Rep. Asahi Glass Found. Ind. Technol.* 1984, 45, 163.
(10) Okahata, Y.; Ando, R.; Kunitake, T. *Ber. Bunsen-Ges. Phys. Chem.* 1981, 85, 789.
(11) Barrer, R. M.; Skirrow, G. *J. Polym. Sci.* 1948, 3, 549.
(12) Hoffman, S. "Depth Profiling" in *Practical Surface Analysis*; Briggs, D.; Seak, M. P., Eds.; Wiley: New York, 1983.
(13) Brundle, C. R. *J. Vac. Sci. Technol.* 1974, 11, 212.
(14) Kajiyama, T.; Nagata, Y.; Washizu, S.; Takayanagi, M. *J. Membr. Sci.* 1982, 11, 39.
(15) Kajiyama, T.; Washizu, S.; Takayanagi, M. *J. Appl. Polym. Sci.* 1984, 29, 3955.
(16) Washizu, S.; Terada, I.; Kajiyama, T.; Takayanagi, M. *Polym. J. (Tokyo)* 1984, 16, 307.
(17) Kajiyama, T.; Washizu, S.; Ohmori, Y. *J. Membr. Sci.* 1985, 24, 73.

Phase Equilibria in Rodlike Systems with Flexible Side Chains[†]

M. Ballauff

Max-Planck-Institut für Polymerforschung, 65 Mainz, FRG. Received July 31, 1985

ABSTRACT: The lattice theory of the nematic state as given by Flory is extended to systems of rigid rods of axial ratio x and appended side chains characterized by the product of z, the number of side chains per rod, and m, the number of segments per side chain. Soft intermolecular forces are included by using the familiar interaction parameter. Special attention is paid to the form of the orientational distribution function, which is introduced in terms of the refined treatment devised by Flory and Ronca as well as in its approximative form given by Flory in 1956. At nearly athermal conditions the theory presented herein predicts a narrowing of the biphasic gap with increasing volume fraction of the side chains. The region where two anisotropic phases may coexist becomes very small in the presence of side chains. It is expected to vanish at a certain critical volume ratio of side chains and rigid core of the polymer molecule. The dense anisotropic phase at equilibrium with a dilute isotropic phase at strong interactions between the solute particles (wide biphasic region) is predicted to become less concentrated with increase of the product of z and m. The deductions of the treatment presented herein compare favorably with results obtained on lyotropic solutions of helical polypeptides like poly(γ-benzyl glutamate).

During recent years there has been a steadily growing interest in thermotropic and lyotropic polymers. Spinning or injection molding in the liquid-crystalline state can lead to fibers of high strength and stiffness.[1] However, the melting point of typical aromatic polyesters exhibiting a mesophase often exceeds 500 °C,[2] which makes the processing of these materials by conventional methods very difficult. In order to reduce the melting temperature of thermotropic polymers, flexible spacers have been inserted between the mesogenic units.[3] But these semiflexible polymers no longer possess the rigidity necessary to produce the desirable mechanical properties.[4] Alternatively, sufficient solubility and lower melting point may be achieved by appending flexible side chains to rigid rod polymers. This third type of liquid-crystalline polymer has been the subject of a number of recent studies. Lenz and co-workers showed that substitution with linear or branched alkyl chains[5,6] considerably lowers the melting point of poly(phenylene terephthalate). Similar observations have been made in the course of a study of poly(3-n-alkyl-4-hydroxybenzoic acids).[7] Gray and co-workers demonstrated that side-chain-modified cellulose derivatives exhibit thermotropic as well as lyotropic behavior.[8,9] The solution properties of poly(γ-benzyl glutamates) (PBLG) are directly influenced by the presence of flexible side chains, as has been pointed out by Flory and Leonard.[10] The thermodynamics of PBLG in various solvents has been investigated theoretically as well as experimentally by Miller and co-workers,[11,12] leading to the conclusion

[†] Dedicated to the memory of Professor P. J. Flory.
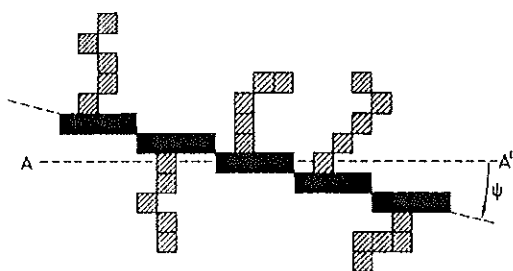
Figure 1. Representation of a rigid rod with appended side chains in a cubic lattice.

that the presence of flexible side chains in this polymer profoundly alters the phase diagrams as compared to the rigid rod model. In this work we present a comprehensive treatment of the thermodynamics of stiff rods with appended flexible side chains. As in the theory of Wee and Miller,[12] it is based on the lattice model originated by Flory,[13,14] which previously has been shown to account for all experimental facts obtained from suitable model systems.[15-19] Special attention is paid to the form of the orientational distribution function, as expressed in terms of the Flory–Ronca theory[20,21] or in the 1956 approximative treatment.[13] In order to treat lyotropic systems soft intermolecular forces are included by means of the familiar interaction parameter. Steric constraints between adjacent side chains appended to the same rod, an important problem in the course of a statistical-mechanical treatment of membranes[22] and semicrystalline polymers,[23] are not taken into account in the present treatment. It is assumed that the distances between neighboring side chains are sufficiently large, as is the case in the polyester systems mentioned above.[5,7] However, as discussed by Flory and Leonard,[10] this effect may come into play when helical polypeptides such as PBLG are considered.

Theory

The system considered here consists of rodlike molecules with flexible side chains appended regularly (cf. Figure 1).

As is customary, we subdivide the lattice into cells of linear dimensions equal to the diameter of the rodlike part of the particle. Thus the number of segments comprising this part is identical with its axial ratio, henceforth denoted by x. For simplicity, we take the segments of the side chains and the molecules of the solvent to be equal in size to a segment of the rodlike part. The axial ratio of the solvent therefore is given by $x_{solvent} = 1$. To each rod z side chains are appended comprising m segments. Since the side chains are not incorporated in the main chain, they are not expected to take part in the course of the ordering transitions. Therefore their configuration may be assumed to remain unaffected by the nature of the respective phase.

Consider a phase or liquid-crystalline domain where the rodlike parts of the molecules are preferentially oriented to the axis of the domain, the latter being taken along one of the principal axes of the lattice. As in ref 13, the stiff part consists of y sequences containing x/y segments (cf. Figure 1). The relation of y to the angle ψ of inclination to the axis of the domain will be discussed later in this section.

The calculation of the configurational partition function rests on the evaluation of the number ν_{j+1} of situations available to the $j + 1$ molecule after j particles are introduced. Let n_0 denote the total number of lattice sites and $f = x + mz$ the overall number of segments per molecule. Pursuant to the calculation of ν_{j+1}, it is expedient to introduce the rigid part first. Doing this we proceed along the lines given in ref 13. The number of situations available to the first segment of the first submolecule thus follows as the number of vacancies $n_0 - fj$. If there is no correlation between the adjacent rows parallel to the axis of the domain, the expectation of a vacancy required for the $y_{j+1} - 1$ first segments of the remaining submolecules is the volume fraction of the vacancies $(n_0 - fj)/n_0$. If a given site for the first segment of a submolecule is vacant, the site following it in the same row can then be only occupied by either the initial segment of a submolecule or a segment of a side chain. The conditional probability therefore is given by the ratio of vacancies to the sum of vacancies, submolecules, and total number of the segments of the side chains $(n_0 - fj)/(n_0 - fj + \sum^j y_i + zmj)$. Inasmuch as we assume that there is no correlation of the conformation of the side chains with the orientational order (see above), the expectancy of a vacancy for the zm segments of the side chains is given by the volume fraction of empty sites $(n_0 - fj)/n_0$. It follows that

$$\nu_{j+1} = (n_0 - fj) \times$$
$$\left(\frac{n_0 - fj}{n_0} \right)^{y_{j+1}-1} \left(\frac{n_0 - fj}{n_0 - fj + \sum\limits^i y_i + zmj} \right)^{x-y_{j+1}} \times$$
$$\left(\frac{n_0 - fj}{n_0} \right)^{zm} \quad (1)$$

or

$$\nu_{j+1} = (n_0 - fj)^f (n_0 - xj + \sum^j y_i)^{y_{j+1}-x} n_0^{1-y_{j+1}-zm} \quad (2)$$

With negligible error we may write

$$\nu_{j+1} = \frac{(n_0 - fj)!}{n_0 - f(j + 1)!} \frac{(n_0 - x(j + 1) + \sum\limits^{j+1} y_i)!}{(n_0 - xj + \sum\limits^j y_i)!} n_0^{1-y_{j+1}-zm} \quad (3)$$

The results deduced by the lattice treatment are expected to become less secure at greater disorientations, i.e., at larger values of y/x. For the ordered phase under consideration here, this problem should be of minor importance, however. As usual,[20] the configurational partition function Z_M may be represented as the product of the combinatorial part Z_{comb}, the orientational part Z_{orient}, and the intramolecular or conformational part Z_{conf}:

$$Z_M = Z_{comb} Z_{orient} Z_{conf} \quad (4)$$

Since the configuration of the side chains is assumed to be independent of the order of the respective phase (see above), Z_{conf} may be dismissed in the subsequent treatment. The combinatorial part is related to ν_j by

$$Z_{comb} = \left(\frac{1}{n_x!} \right) \prod^{n_x} \nu_j \quad (5)$$

and thus follows as

$$Z_{comb} = \frac{(n_0 - n_x x + \bar{y} n_x)!}{n_x! n_1!} n_0^{n_x(1-\bar{y}-zm)} \quad (6)$$

where $n_1 = n_0 - fn_x$ denotes the number of solvent particles and n_x the number of polymer molecules. As usual, $\bar{y}$ is the average value of the disorder index y defined by

$$\bar{y} = \sum \frac{n_{xy}}{n_x} y \quad (7)$$

with n_{xy} being the number of molecules whose rigid core is characterized with regard to orientation by y. Following

Flory and Ronca,[20] the orientational part of Z_{orient} becomes

$$Z_{orient} = \prod_y \left(\frac{\sigma \omega_y n_x}{n_{xy}} \right)^{n_{xy}} \tag{8}$$

As in ref 20, ω_y denotes the a priori probability for the interval of orientation related to y, and σ is a constant. Introducing Stirling's approximation for the factorials, eq 4 together with eq 5 and 6 gives

$$-\ln Z_M = n_1 \ln v_1 + n_x \ln \frac{v_x}{x} -$$
$$(n_0 - n_x x + \bar{y} n_x) \ln \left[1 - v_x \left(1 - \frac{\bar{y}}{x} \right) \right] -$$
$$n_x (1 - \bar{y} - zm) + n_x \sum_y \frac{n_{xy}}{n_x} \ln \left[\frac{n_{xy}}{n_x} \frac{1}{\omega_y} \right] - n_x \ln \sigma \tag{9}$$

where the quantities $v_1 = n_1/n_0$ and $v_x = n_x x/n_0$ denote the volume fractions of the solvent and of the rigid core of the polymer, respectively.

For evaluating the orientational distribution we take the last molecule inserted into the lattice as a probe for the orientational order at equilibrium (see ref 20). Hence, equating $j + 1$ in eq 2 to n_x, we obtain

$$\nu_y \sim \left(1 - v_x \left(1 - \frac{\bar{y}}{x} \right) \right)^y \tag{10}$$

which immediately leads to

$$n_{xy}/n_x = f_1^{-1} \omega_y \exp(-ay) \tag{11}$$

with the quantity a defined by

$$a = -\ln \left[1 - v_x \left(1 - \frac{\bar{y}}{x} \right) \right] \tag{12}$$

and

$$f_1 = \sum_y \omega_y \exp(-ay) \tag{13}$$

Alternatively, eq 11 may be derived by variational methods.[20] Note that the orientational distribution function n_{xy}/n_x is given by the same expression as deduced in ref 20. Thus the functional dependence of n_{xy}/n_x on the disorientation index y of the rodlike part remains unaffected by the presence of flexible side chains. Accordingly, Z_{orient} follows as

$$Z_{orient} = n_x [\ln (f_1 \sigma) + a\bar{y}] \tag{14}$$

and, upon insertion into (9)

$$-\ln Z = n_1 \ln v_1 + n_x \ln \frac{v_x}{x} - (n_0 - n_x x) \ln \left[1 - v_x \left(1 - \frac{\bar{y}}{x} \right) \right] - n_x (1 - \bar{y} - zm) - n_x \ln (f_1 \sigma) \tag{15}$$

For examining the effect of small interactions between the solute particles, the heat of mixing ΔH_M is incorporated into the expression for the free energy. If it is assumed that randomness of mixing is preserved at all degrees of orientation, ΔH_M may be taken to be proportional to the number of segments of one type and the volume fraction of the other species. Hence, introducing the familiar interaction parameters χ_{12}, χ_{13}, and χ_{23}, ΔH_M becomes

$$\Delta H_M = \chi_{12} n_1 v_2 + \chi_{13} n_1 v_s + \chi_{23} n_2 v_3 \tag{16}$$

where the index 1 refers to the solvent, 2 to the rigid part

of the solute particle, and 3 to the flexible side chains. The quantities χ_{ij} are given as usual[24] by

$$\chi_{ij} = Z_c \Delta w_{ij} x_j / RT \tag{17}$$

where x_j represents the number of segments per interacting species, Z_c is the coordination number, and Δw_{ij} ($= w_{ij} - 0.5(w_{ii} + w_{jj})$) denotes the change in energy for the formation of an unlike contact. Since the volume fraction v_s of the side chains depends on v_x through $v_s = v_x zm/x$, we have

$$\Delta H_M = \chi_1 n_1 v_x + \chi_2 n_x v_x \tag{18}$$

with

$$\chi_1 = \chi_{12} + \frac{zm}{x} \chi_{13} \tag{19}$$

and

$$\chi_2 = \frac{zm}{x} \chi_{23} \tag{20}$$

The chemical potentials are derived from eq 7 and 18 with the stipulation that at orientational equilibrium

$$\left(\frac{\ln Z_M}{(n_{xy}/n_x)} \right)_{n_1, n_x} = 0$$

Hence

$$\Delta \mu_1'/RT = \ln v_1 + v_s' + \frac{v_x'}{x}(y - 1) + a +$$
$$v_x' \left[(v_x' + v_s') \chi_1 - \frac{v_x'}{x} \frac{zm}{x} \chi_2 \right] \tag{21}$$

and

$$\Delta \mu_x'/RT = \ln \frac{v_x'}{x} - f \left(v_1' + \frac{v_x'}{x} \right) + f - v_x' f \left(1 - \frac{\bar{y}}{x} \right) +$$
$$zma - \ln (f_1 \sigma) + \left(1 - v_x' \frac{f}{x} \right) \left(v_1' x \chi_1 + v_x' \frac{zm}{x} \chi_2 \right) \tag{22}$$

In what is to follow all quantities referring to the anisotropic phase are marked by a prime. The corresponding expressions for the isotropic phase, obtained by equating y to x, are

$$\Delta \mu_1/RT =$$
$$\ln v_1 + v_s + v_x \left(1 - \frac{1}{x} \right) + v_x \left[(v_x + v_s) \chi_1 - \frac{v_x}{x} \frac{zm}{x} \chi_2 \right] \tag{23}$$

$$\Delta \mu_x/RT = \ln \frac{v_x}{x} + f + f \left(v_1 + \frac{v_x}{x} \right) - \ln \sigma +$$
$$\left(1 - v_x \frac{f}{x} \right) \left(v_1 x \chi_1 + v_x \frac{zm}{x} \chi_2 \right) \tag{24}$$

For evaluating the composition of the conjugated phases by means of the equilibrium conditions

$$\Delta \mu_1 = \Delta \mu_1' \tag{25}$$
$$\Delta \mu_2 = \Delta \mu_2' \tag{26}$$

the relation between y and the angle of inclination has to be specified. Since the orientational distribution as represented by eq 11 does not change when flexible side chains are appended to the stiff rods, we may directly use the expression given by the Flory–Ronca treatment of the lattice model.[20] Thus the disorder index y is represented by

$$y = \frac{4}{\pi} x \sin \psi \qquad (27)$$

In orientational equilibrium its average value follows as

$$\bar{y} = \frac{4}{\pi} x f_2 / f_1 \qquad (28)$$

and the order parameter s becomes

$$s = 1 - \tfrac{3}{2} f_3 / f_1 \qquad (29)$$

with the integrals f_p being given by

$$f_p = \int_0^{\pi/2} \sin^p \psi \, \exp(-\alpha \sin \psi) \, d\psi \qquad (30)$$

The factor α relates to a (cf. eq 12) by

$$\alpha = \frac{4}{\pi} a x \qquad (31)$$

For values of $\alpha \gg \pi/2$, the integrals f_p may be developed in series, yielding

$$f_1 = \frac{1}{\alpha^2} + \mathcal{O}\!\left(\frac{1}{\alpha^4}\right) \qquad (32)$$

$$f_2 = \frac{2}{\alpha^3} + \mathcal{O}\!\left(\frac{1}{\alpha^5}\right) \qquad (33)$$

$$f_3 = \frac{6}{\alpha^4} + \mathcal{O}\!\left(\frac{1}{\alpha^6}\right) \qquad (34)$$

In this asymptotic approximation[20] the average disorder parameter $\bar{y}$ directly follows from

$$\bar{y} = \frac{2}{a} = -\frac{2}{\ln\,[1 - v_x(1 - \bar{y}/x)]} \qquad (35)$$

Thus, we obtain for the chemical potentials eq 23 and 24 the expressions

$$\Delta\mu_1'/RT = \ln v_1' + v_s' + \frac{v_x'}{x}(\bar{y} - 1) + \frac{2}{\bar{y}} +$$
$$v_x'\left[(v_x' + v_s')\chi_1 - \frac{v_x'}{x}\frac{zm}{x}\chi_2 \right] \qquad (36)$$

$$\Delta\mu_x'/RT =$$
$$\ln \frac{v_x'}{x} - f\!\left(v_1' + \frac{v_x'}{x}\right) + f - v_x'\!\left(1 - \frac{\bar{y}}{x}\right) + \frac{2zm}{\bar{y}} + 2(1 -$$
$$\ln \bar{y}) - \ln \frac{\sigma}{x^2} - C + \left(1 - v_x'\frac{f}{x}\right)\!\left[v_1'x\chi_1 + v_x'\frac{zm}{x}\chi_2 \right] \qquad (37)$$

where $C = 2 \ln (\pi e/8)$. Further simplification can be achieved by omitting the small constant C and equating σ to x (1956 approximation; cf. ref 11). In order to obtain the volume fraction of the polymer in the coexisting phases, trial values of v_x' and a (cf. eq 12) are chosen which serve for the numerical evaluation of the integrals f_p through eq 30. If the quantity α (eq 31) exceeds 30, the f_p may be calculated by the series expansion eq 32–34 using the first four terms. With the f_p being known, $\bar{y}$ follows from (28), which in turn leads to an improved value of a. The whole calculation is repeated until self-consistency is reached. Equation 26 is then solved numerically to obtain v_x, from which an improved value of v_x' is accessible via eq 25. The entire calculation is repeated with a new value of v_x' until compliance with all conditions for equilibrium is reached. When the 1956 approximation is used, the same scheme

applies to eq 25 and 26, with eq 21 and 22 being replaced by eq 36 and 37. Here, self-consistency directly follows from eq 35. The volume fractions v_x' and v_x'' of two anisotropic phases in equilibrium can be evaluated by a similar numerical solution of (25) and (26) after insertion of (21) and (22) together with (28). Since this calculation is more sensitive toward the orientational distribution function, the exact treatment of Z_{orient} has to be used.

Results and Discussion

Parts a–d of Figure 2 show the phase diagrams resulting for rigid rods of axial ratio $x = 100$ with flexible side chains characterized by the number of side chains z per rod and the number of segments m per side chain.

From the theoretical treatment it is evident that only the product zm matters. Thus the polymer molecules under consideration here are fully determined by x and zm. Since the segments of the side chains are assumed to be isodiametric with the segments of the rigid core, the quantity zm/x directly gives the ratio of the volumes occupied by the respective parts of the molecule. For the present purpose of a discussion of the influence exerted by the side chains, the parameter χ_1 (see eq 19) measuring the interaction of the solvent and the rigid core will suffice to take into account intermolecular forces. The second parameter χ_2 related to the interactions of the side chains with the rigid core only matters at very high concentrations and is thus of minor importance.

Figure 2a corresponds to a system of rigid rods immersed in a solvent. The dashed lines indicate the metastable continuations of the phase lines. This diagram has been calculated by Flory in the famous work[13] in 1956 using the approximate form of the orientational distribution (see eq 36–38). The result given herein was obtained by resort to the treatment of the lattice model originated by Flory and Ronca.[20] A comparison of both methods shows that the main features of the diagram are rather insensitive toward the respective form of the orientational distribution function n_{xy}/n_x. However, the stability of the equilibria between two nematic phases is profoundly influenced by n_{xy}/n_x. This fact becomes even more important when going to lower axial ratios x. For example, the Flory–Ronca treatment predicts a triphasic equilibrium already for $x = 50$, an axial ratio not being sufficient to produce a stable nematic–nematic equilibrium in the frame of the 1956 approximation. From these results it is obvious that the exact treatment of n_{xy}/n_x is necessary for the precise calculation of the triphasic equilibria but is sufficiently accurate for evaluating the isotropic–nematic equilibrium at axial ratios greater than 100.

As can be seen from a comparison of Figure 2, part a, with parts b–d, there is a marked influence of the side chains on the phase behavior of rigid rods. We first discuss Figure 2, part a, 2a together with part b referring to $zm = 0$ and $zm = 2$, respectively. Here v_p and v_p' denote the total volume fractions of the polymer in the isotropic phase and in the coexisting ordered phase. Both phase diagrams exhibit the same gross features. At $\chi_1 = 0$ the soft interactions between the rods and the solvent are null, corresponding to athermal conditions. The narrow biphasic region at this point is continued until a pair of reentrant nematic phases appears at a critical point noted on the right-hand side of the ordinate. At a given value of χ_1, in the regime just beyond the critical point, either of two pairs of phases n,i or n,n may occur. Further increase of χ_1, equivalent to a lowering of temperature, leads to a triple point where three phases are in equilibrium. Raising χ_1 to still higher values is followed by a dilute isotropic phase in equilibrium with a dense nematic phase.
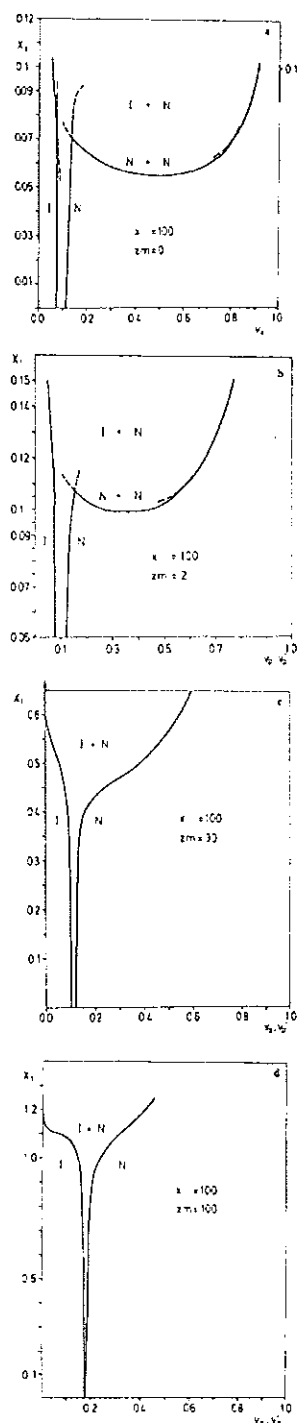
Figure 2. Phase diagrams of rigid rods immersed in a solvent; x is the axial ratio of the rigid core, z is the number of side chains per rigid core, and m is the number of segments per side chain. The solvent power is measured by the interaction parameter χ_1. The quantities v_p and v_x denote the volume fraction of the total polymer and its rigid core, respectively.

Several features command attention when Figure 2, parts a and b, are compared. Going from $zm = 0$ (perfectly rigid rods) to $zm = 2$ narrows considerably the region where two nematic phases are coexisting. If $zm > 4$, this region be-
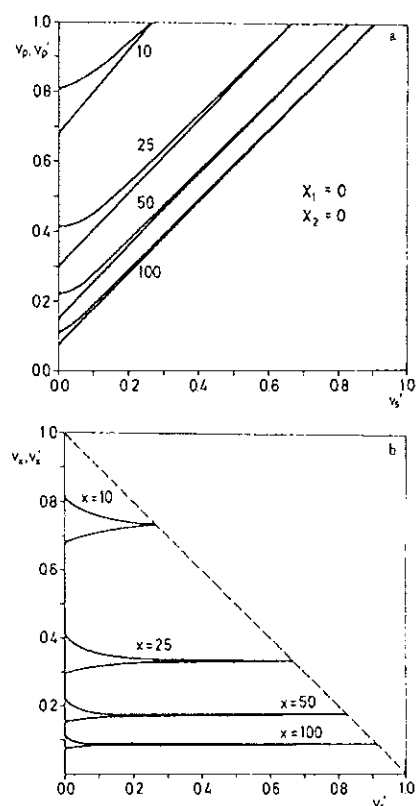

Figure 3. (a) Volume fraction v_p and v_p' of the polymer in the coexisting isotropic and anisotropic phase, respectively, at athermal conditions vs. the volume fraction v_s' of side chains in the anisotropic phase. (b) Volume fraction v_x and v_x' of the polymer in the coexisting isotropic and anisotropic phase, respectively, at athermal conditions vs. the volume fraction v_s' of side chains in the antisotropic phase.

comes unstable for $x = 100$. Note that both the critical value of χ_1 and its value at the triple point are increasing with appending of side chains. Furthermore, the anisotropic phase coexisting with the isotropic phase above the critical point is less concentrated when compared to $zm = 0$. Thus, even a small volume fraction of side chains as expressed by the ratio of zm to x suffices to change the phase behavior profoundly. This is even more obvious when higher values of zm (Figure 2c,d) are used. Here, the triphasic equilibrium is no longer stable. In addition, the widening of the biphasic gap occurs at much higher values of χ_1, as compared to rods without side chains (cf. Figure 2a; note the different scales of the ordinate in Figure 2a–d). Hence, the wide biphasic regime is expected to appear at a much lower temperature. Another feature of interest is the narrowing of the two-phase region with increase of zm at constant x. For athermal conditions this is shown in more detail in Figure 3a.

Here the volume fractions v_p and v_p' in the respective phases are plotted against the volume fraction v_s' of the side chains in the anisotropic phase. It is evident that appending of even short chains results in a strong narrowing of the biphasic gap. This effect is most pronounced at higher axial ratios x where the two-phase region becomes negligible if $v_s' > v_x'$. Figure 3b shows the respective volume fractions v_x and v_x' of the rigid core of the polymer. As is obvious from this plot, the presence of flexible side chains changes the width of the biphasic gap but leaves the magnitude of v_x nearly unaffected. Clearly, as in Figure

DOCKET ALARM

Explore Litigation Insights

Docket Alarm provides insights to develop a more informed litigation strategy and the peace of mind of knowing you're on top of things.

Real-Time Litigation Alerts

Keep your litigation team up-to-date with **real-time alerts** and advanced team management tools built for the enterprise, all while greatly reducing PACER spend.

Our comprehensive service means we can handle Federal, State, and Administrative courts across the country.

Advanced Docket Research

With over 230 million records, Docket Alarm's cloud-native docket research platform finds what other services can't. Coverage includes Federal, State, plus PTAB, TTAB, ITC and NLRB decisions, all in one place.

Identify arguments that have been successful in the past with full text, pinpoint searching. Link to case law cited within any court document via Fastcase.

Analytics At Your Fingertips

Learn what happened the last time a particular judge, opposing counsel or company faced cases similar to yours.

Advanced out-of-the-box PTAB and TTAB analytics are always at your fingertips.

API

Docket Alarm offers a powerful API (application programming interface) to developers that want to integrate case filings into their apps.

LAW FIRMS

Build custom dashboards for your attorneys and clients with live data direct from the court.

Automate many repetitive legal tasks like conflict checks, document management, and marketing.

FINANCIAL INSTITUTIONS

Litigation and bankruptcy checks for companies and debtors.

E-DISCOVERY AND LEGAL VENDORS

Sync your system to PACER to automate legal marketing.